
Rethinking the Principle of Gradient Smooth Methods in Model Explanation

Linjiang Zhou

School of Cyber Science and Engineering
Wuhan University
Wuhan, China 430072
linjiang@whu.edu.cn

Chao Ma

School of Cyber Science and Engineering
Wuhan University
Wuhan, China 430072
chaoma@whu.edu.cn

Zepeng Wang

School of Cyber Science and Engineering
Wuhan University
Wuhan, China 430072
wangzepeng@whu.edu.cn

Xiaochuan Shi*

School of Cyber Science and Engineering
Wuhan University
Wuhan, China 430072
shixiaochuan@whu.edu.cn

Abstract

Gradient Smoothing is an efficient approach to reducing noise in gradient-based model explanation method. SmoothGrad adds Gaussian noise to mitigate much of these noise. However, the crucial hyper-parameter in this method, the variance σ of Gaussian noise, is set manually or with heuristic approach. However, it results in the smoothed gradients still containing a certain amount of noise. In this paper, we aim to interpret SmoothGrad as a corollary of convolution, thereby re-understanding the gradient noise and the role of σ from the perspective of confidence level. Furthermore, we propose an adaptive gradient smoothing method, AdaptGrad, based on these insights. Through comprehensive experiments, both qualitative and quantitative results demonstrate that AdaptGrad could effectively reduce almost all the noise in vanilla gradients compared with baselines methods. AdaptGrad is simple and universal, making it applicable for enhancing gradient-based interpretability methods for better visualization.

1 Introduction

Explanation for deep learning model is a critical part of Artificial Intelligence (AI) applications with human interaction. For instance, explanation methods are crucial in these data-sensitive and decision-sensitive fields like medical image analysis [4], financial data analysis [48] and autonomous driving [1]. Additionally, given the prevalence of personal data protection laws in most countries and regions, fully black-box AI models may face intense legal scrutiny [14].

In recent years, some explanation methods have attempted to explain neural network decisions by visualizing the decision rationale and feature importance [30]. These local explanation techniques aim to provide explanations for individual samples. Moreover, the explanation process of these methods often leverage the gradients of the neural network. For instance, Grad-CAM [33], Grad-CAM++ [11], and Score-CAM [42] utilize gradients to generate the weight of class activation maps.

Gradients of input samples are the critical information for analyzing the deep neural networks [39]. However, these gradients often contain a significant amount of noise. This is due to the complex

*Corresponding author

structure and numerous parameters in neural networks [29]. As mentioned in [2, 24, 46], these noise could severely affect the explanation method on mining the latent learning features. Moreover, caused by both local noise and gradient saturation, the sample gradients could not accurately explain the influence of sample values on model decisions [40]. Therefore, smoothing out the noise in gradients is an important approach to improve the interpretability of the model.

SmoothGrad [38] is currently the most widely applied and empirically proven simplest yet effective method for gradient smoothing. Although other methods like NoiseGrad [9] have also been proposed for gradient smoothing. SmoothGrad, because of its universality and practicality, is almost the only gradient smoothing method extensively used in model explanation. However, as mentioned in [5, 31, 9, 30], the principles behind SmoothGrad for noise eliminate have not been thoroughly discussed. Furthermore, its key parameter σ , the variance of Gaussian noise, is set empirically. As proven in our paper, σ almost determines the noise elimination capability of SmoothGrad. Moreover, we found that even when the SmoothGrad method reaches its theoretical limit, a certain amount of noise still exists in the smoothed gradients. The remained noise significantly impairs the visualization capability of gradients to interpret model features.

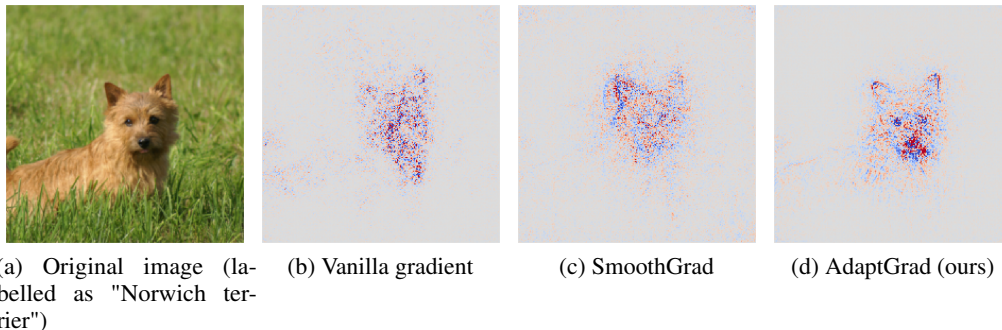


Figure 1: An example to compare the visual performance between different gradient smoothing methods.

In this paper, we rethink the fundamental principles in SmoothGrad by utilizing the convolution formula, thus re-understand its critical parameters. This allows us to theoretically analyze the shortcomings of SmoothGrad and subsequently design an adaptive gradient smoothing method, AdaptGrad. Figure 1 illustrates an example of AdaptGrad. We not only theoretically prove that AdaptGrad outperforms SmoothGrad, but also demonstrate that our AdaptGrad is capable of eliminating almost all the noise while the smoothed gradients revealing richer detail features. Similar to SmoothGrad, AdaptGrad is also simple and universal, making it applicable for enhancing gradient-based interpretability methods. Also, we comprehensively demonstrate the superiority of AdaptGrad through experiments with other gradient-based interpretability methods.

2 Related Work

In general, consider a neural network as a function $F(\mathbf{x}; \theta) : \mathbb{R}^D \rightarrow \mathbb{R}^C$ with the trainable parameters θ and its output could be the probability, logit, etc. D is the input dimension of the neural network, and C is the output dimension. In the example of a classification function, the neural network will output a score for each class c , where $c \in \{1, \dots, C\}$. When further considering only the output of the neural network in a single class c , the neural network can be simplified to a function $F^c(\mathbf{x}; \theta) : \mathbb{R}^D \rightarrow \mathbb{R}$, which maps the input \mathbb{R}^D to the 1-dimension \mathbb{R} space. For simplicity, we use $F(\mathbf{x})$ to represent the neural network and only consider the output of the neural network on a single class c .

The gradient of $F(\mathbf{x})$ could be presented as shown in Equation 1.

$$G(\mathbf{x}) = \frac{\partial F(\mathbf{x})}{\partial \mathbf{x}}. \quad (1)$$

A possible explanation [29] for the large amount of noise in the original gradient is that considering the local surroundings of a sample, neural networks tend not to present an ideal linearity but rather

have a very rough and nonlinear decision boundary. So the complexity of neural networks and the input features usually leads to the unreliability of the vanilla sample gradients.

Similarly, gradient maps like those in Figure 1 are commonly referred to as saliency maps or heatmaps. For simplicity, this paper uniformly refers to them as saliency maps and also refers to the results generated by other explanation methods as saliency maps. The highlighted areas in these maps indicate the relevant features learned by the neural network or the basis for the decisions.

The methods for reducing gradient noise can be roughly categorized into the following two groups:

Adding noise to reduce noise. SmoothGrad proposed by [38] introduces stochasticity to smooth the noisy gradients. SmoothGrad averages the gradients of random samples in the neighborhood of the input \mathbf{x}_0 . This could be formulated as shown in Equation 2.

$$G_{sg}(\mathbf{x}) = \frac{1}{N} \sum_i^N G(\mathbf{x} + \varepsilon), \varepsilon \sim \mathcal{N}^D(0, \Sigma_{sg}), \Sigma_{sg} = I_D * \sigma^2 \quad (2)$$

In Equation 2, N is the sample times, and ε is distributed over D -dimension $\mathcal{N}^D(0, \Sigma_{sg})$. Similar to SmoothGrad, NoiseGrad and FusionGrad presented in [9] additionally add perturbations to model parameters. And the FusionGrad is a mixup of NoiseGrad and SmoothGrad. These simple methods are experimentally verified to be efficient and robust [13].

Improving backpropagation to reduce noise. Deconvolution [47] and Guided Backpropagation [39] directly modify the gradient computation algorithm of the ReLU function. Integrate Gradient (IG) [40] was proposed to replace the original gradient for interpretation, and proved to have axiomatic completeness. Some other methods such as Feature Inversion [15], Layerwise Relevance Propagation [7], DeepLift [34], Occlusion [5], Deep Taylor [29] employ some additional features to approximate or improve the gradient for precise visualization.

3 Convolution for Smoothing

SmoothGrad is a simple yet effective gradient smoothing method. However, some of its underlying principles have not been fully discussed. As discussed in [9], SmoothGrad is essentially a Monte Carlo method. Following the discussion, we could further derive the definition of SmoothGrad to gain a deeper understanding.

3.1 Monte Carlo Approximation for Convolution

As we described in Section 2, SmoothGrad is formulated in Equation 2. By performing a simple transformation of the summation part, SmoothGrad could be redefined as Equation 3.

$$G_{sg}(\mathbf{x}) = \frac{1}{N} \sum_i^N G(\mathbf{x} + \varepsilon) = \frac{1}{N} \sum_i^N \frac{G(\mathbf{x} + \varepsilon)p(\varepsilon)}{p(\varepsilon)} \quad (3)$$

In Equation 3, the $p(\cdot)$ is the Probability Density Function (PDF) function of D -dimension distribution $\mathcal{N}^D(0, \Sigma_{sg})$. Furthermore, according to the Monte Carlo integration principle, the limit of G_{sg} can be estimated as N approaches infinity (sampling an infinite number of times). So we could obtain the upper limit in Equation 4.

$$\lim_{N \rightarrow \infty} G_{sg}(\mathbf{x}) = \lim_{N \rightarrow \infty} \frac{1}{N} \sum_i^N \frac{G(\mathbf{x} + \varepsilon)p(\varepsilon)}{p(\varepsilon)} = \int G(\mathbf{x} + \varepsilon)p(\varepsilon)d\varepsilon = (G * p)(\mathbf{x}) \quad (4)$$

In Equation 4, the $*$ is the convolution operator. So we redefine SmoothGrad as shown in Equation 5.

$$G_{sg}(\mathbf{x}) \simeq (G * p)(\mathbf{x}), p = PDF(\mathcal{N}^D(0, \Sigma_{sg})) \quad (5)$$

In this way, we establish a mathematical connection between σ and the smoothed gradient G_{sg} . That is, σ determines Σ_{sg} and the function $p(\cdot)$, which in turn determines the convolution result $(G * p)(\cdot)$, and further determines the convergence value of G_{sg} as the number of sampling times increases.

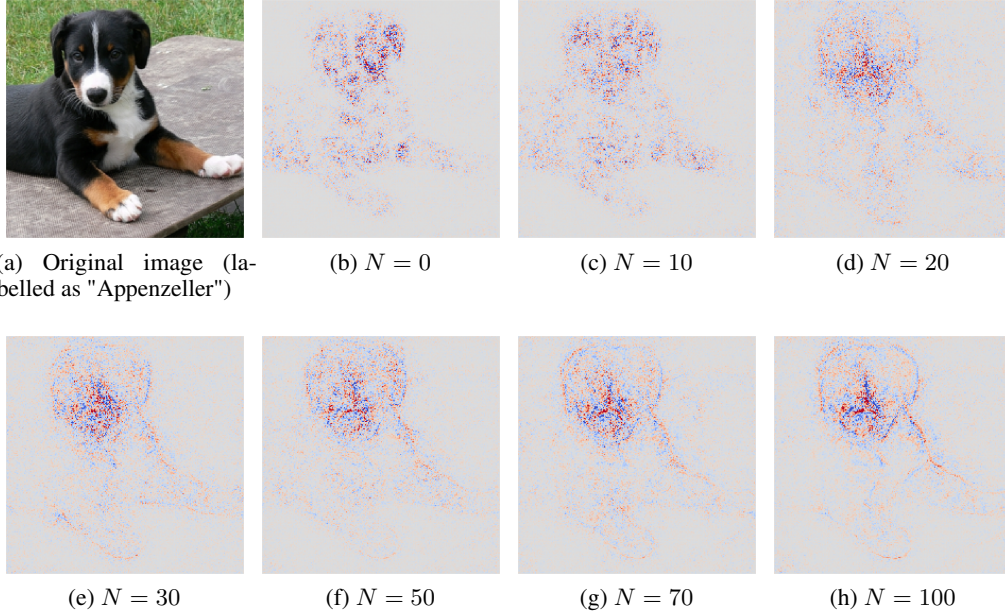


Figure 2: The visual saliency map G_{sg} of SmoothGrad with different sampling number N and $\sigma = 0.2 \times (x_{max} - x_{min})$. The classification model is VGG16 [35], and this image is from ILSVRC2012 [25].

3.2 Noise in the Smoothed Gradient

As implied by Equation 5, when the sampling number N is sufficiently large, G_{sg} has an upper limit. As shown in Figure 2, we present a visual example of SmoothGrad in image classification. As N increases, around 50 to 70, G_{sg} gradually converges. However, even as G_{sg} approaches the smooth upper limit, the residual noise in G_{sg} could still affect the details in the saliency map. In the example of Figure 2, when $N = 100$, in the facial area of the dog, it still makes it difficult to discern the detailed features, and there are still a certain amount of noise points at the edges of the target.

According to our discussion in Section 4, the variance σ , also the the variance of Gaussian noise in SmoothGrad, determines the limit of G_{sg} . SmoothGrad employs a simple strategy to select an appropriate value for σ . Assume that the minimum value of the input data is denoted as x_{min} and the maximum value as x_{max} . SmoothGrad introduces a new variable α (set to 0.2 as recommended by [38]) to compute σ . The relationship between them is expressed in Equation 6.

$$\sigma = \alpha \times (x_{max} - x_{min}) \quad (6)$$

However, we believe that this setup leads to a significant amount of residual noise in G_{sg} . In fact, what SmoothGrad ignored is that the integral in Equation 4 which is not performed over \mathbb{R}^D , but rather there is an upper and lower bound according to the statistical features of the dataset, that is, $[x_{min}, x_{max}]$. Therefore, after incorporating the integral region into Equation 4, the G_{sg} could be redefined to Equation 7.

$$G_{sg}(\mathbf{x}) \simeq \int_{\Omega} G(\mathbf{x} + \varepsilon)p(\varepsilon)d\varepsilon, \quad \Omega = \{[x_i] | x_i \in [x_{min}, x_{max}]\} \quad (7)$$

Clearly, in Equation 7, the domains of $G(\cdot)$ and $p(\cdot)$ are inconsistent. The former is Ω while the latter is \mathbb{R}^D . The values of input samples beyond the bounds of Ω should be considered meaningless. Therefore, during smoothing, SmoothGrad would sample some values that are out of Ω . It is precisely that this "out-of-bounds" behavior of SmoothGrad leads to the persistence of a significant amount of noise in G_{sg} .

The noise in saliency map calculated with SmoothGrad is consist of two parts, the original noise in gradient and inherent noise caused by the out-of-bound samples. As described in Figure 2, the former gradually decreases with the increase of the sample times, while the latter is an inherent defect of the SmoothGrad method. Therefore, we define the noise caused by sampling out of bounds as the inherent noise.

Furthermore, we define the inherent noise quantitatively as the probability value of sampling points exceeding the domain of the dataset in gradient smoothing methods. In this way, we can mathematically express the inherent noise in SmoothGrad.

Given an input sample $\mathbf{x} = [x_1, x_2, \dots, x_D] \in \Omega$, for simplicity, we only focus on one variable x_i of \mathbf{x} . Clearly, for the one-dimensional case, the smoothed gradient G_{sg}^i of the gradient with respect to the variable x_i can be represented in Equation 8.

$$G_{sg}^i \simeq \int_{x_{min}}^{x_{max}} G(x_i + \varepsilon_i; \mathbf{x} \setminus x_i) p(\varepsilon_i) d\varepsilon_i, \varepsilon_i \sim \mathcal{N}(0, \sigma^2), p = PDF(\mathcal{N}(0, \sigma^2)) \quad (8)$$

Notice that $x_i + \sigma$ is also a random variable and follows the distribution $\mathcal{N}_{x_i, \sigma}$. Therefore, we quantitatively define inherent noise is the probability that $x_i + \sigma$ is out of $[x_{min}, x_{max}]$. The intrinsic noise on the i -th dimension A^i can be expressed as Equation 9.

$$A^i = 1 - \int_{x_{min} - x_i}^{x_{max} - x_i} p(t) dt \quad (9)$$

The inherent noise of SmoothGrad could be presented by the probability A_{sg}^i (integral area), which could be defined in Equation 10, where $\text{erf}(\cdot)$ is the Error Function.

$$A_{sg}^i = 1 - \frac{1}{2} \text{erf}\left(\frac{x_{max} - x_i}{\sqrt{2}\alpha(x_{max} - x_{min})}\right) + \frac{1}{2} \text{erf}\left(\frac{x_{min} - x_i}{\sqrt{2}\alpha(x_{max} - x_{min})}\right) \quad (10)$$

In Figure 3, we provide a simple example of the simulated value of intrinsic noise A_{sg} . To intuitively highlight the presence of inherent noise, we designed a simple experiment for observation. We randomly selected 1,000 images from the ILSVRC2012 dataset, setting the hyperparameter sampling number $N = 50$ and the $\alpha = 0.2$ in SmoothGrad (following the setting in [38]). We recorded two metrics: the probability of out-of-bounds samples occurring at the image level in a single image, and the probability of out-of-bounds samples occurring at the individual pixel level. The probability value of the former is $100\% \pm 0.00\%$, while that of the latter is $12.62\% \pm 0.01\%$. This indicates that almost every saliency map generated by SmoothGrad contains inherent noise, with a proportion as high as $12.62\% \pm 0.01\%$.

4 Adapted Sampling to Reduce Noise

The inconsistency between the noise sampling distribution and the domain of the input data leads to the fact that the smoothed gradient still retains a certain amount of noise. Therefore, we propose a gradient smoothing method called AdaptGrad, which adaptively adjusts the noise sampling distribution according to the input data, to alleviate this problem and significantly improve the performance of the gradient smoothing.

According to the analysis in Subsection 3.2, our goal is to control the intrinsic noise. Therefore, one of the most direct methods is to set a minimum upper limit on the amount of intrinsic noise. In fact, this goal is similar to parameter estimation parameters under a given confidence level. Therefore, we design a new gradient smoothing method, AdaptGrad, to calculate the smoothed gradient G_{ag} with a given confidence level c . The G_{ag} could be computed as Equation 11-Equation 13, where $\text{erfinv}(\cdot)$ is the Inverse Error Function and diag means the diagonal matrix.

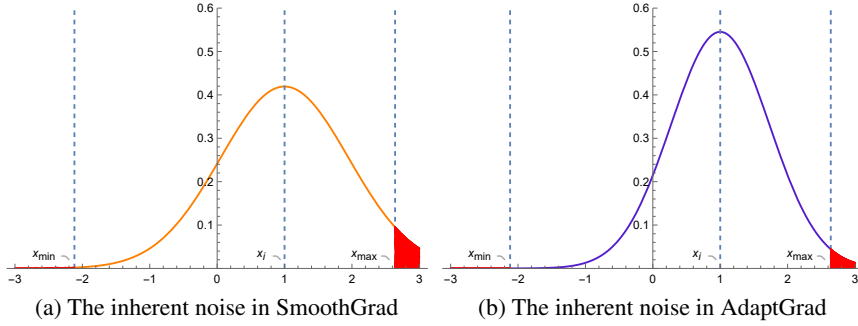


Figure 3: An example to show the inherent noise in gradient smooth. The red area represents the inherent noise (A_{sg} and A_{ag}). In this example, x_{min} is set to -2.12 , x_{max} is set to 2.64 (referring to ILSVR2012), and x_i is assumed to follow a uniform distribution. For SmoothGrad, α is set to 0.2 , and the expected area is 0.1596 . For AdaptGrad, c is set to 0.95 , and the expected area is 0.01424 .

$$G_{ag} = \frac{1}{N} \sum_i^N G(\mathbf{x} + \epsilon), \epsilon \sim \mathcal{N}^D(0, \Sigma_{ag}) \quad (11)$$

$$\Sigma_{ag} = \text{diag}(\sigma_1^2, \sigma_2^2, \dots, \sigma_D^2) \quad (12)$$

$$\sigma_i = \frac{\min(|x_i - x_{min}|, |x_i - x_{max}|)}{\sqrt{2}\text{erfinv}(\frac{1+c}{2})} \quad (13)$$

To explain the design idea of AdaptGrad, we still focus on one variable x_i . We aim to calculate σ_i to make the random variable $x_i + \epsilon_i$ being within the given confidence interval $[x_{min}, x_{max}]$ at a confidence level of c . This means that we directly set the maximum value of inherent noise to $1 - c$. So, we need to solve the variable σ_i in Equation 14.

$$1 - \underbrace{\frac{1}{2}\text{erf}\left(\frac{x_{max} - x_i}{\sqrt{2}\sigma_i}\right) + \frac{1}{2}\text{erf}\left(\frac{x_{min} - x_i}{\sqrt{2}\sigma_i}\right)}_{A_{ag}^i} = c \quad (14)$$

However, the σ_i in Equation 14 does not exist a simple analytical solution, making it nearly impossible to implement the corresponding algorithm in practice. Therefore, by taking the advantage of the symmetry of the normal distribution, we define the confidence interval as $[-\min(|x_{max} - x_i|, |x_{min} - x_i|), \min(|x_{max} - x_i|, |x_{min} - x_i|)]$. This means that the half-length of the interval is determined by the shortest distance from x_i to the boundaries. Therefore, we can obtain the σ_i from Equation 13. In extended case of D -dimensions, we construct the covariance matrix Σ_{ag} , thereby reducing the noise caused by out-of-bounds behavior via sampling from the distribution $\mathcal{N}^D(0, \Sigma_{ag})$.

In AdaptGrad, the confidence level c can follow the definition of low-probability events in probability theory, and is set to 0.95 , 0.99 , 0.995 , 0.999 , etc. Figure 3 shows a simple example to quantitatively illustrate that the inherent noise of AdaptGrad is less than that of SmoothGrad. Figure 4 then shows the visual performance of AdaptGrad under different confidence levels. In fact, the smaller the value of σ (the larger the value of c) is, the more the original noise, but the less the inherent noise. Therefore, we recommend setting $c = 0.95$, and apply this setting in all following evaluation.

5 Experiments

In this section, we evaluate AdaptGrad and baseline methods from both qualitative and quantitative perspectives, as well as its performance when combined with other explanation methods.

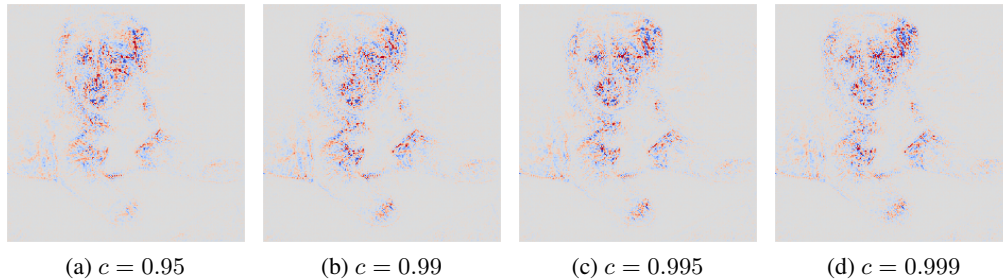


Figure 4: The visual saliency map G_{ag} of AdaptGrad with different confidence level c . Other settings are the same as Figure 2.

5.1 Experimental Settings

All experimental codes and saved model parameters with detailed results can be found in the Supplementary Material, and will be released on the public code platform under anonymous policy.

5.1.1 Metrics

Gradient smoothing methods are often applied as explanation techniques in the field of computer vision. Therefore, the visualization performance is an important metric for evaluating the performance of these methods. However, there is currently a lack of an unified method to objectively quantify the visualization performance. So, we aim to provide a set of visualization examples in Subsection 5.2 to objectively demonstrate the effectiveness of AdaptGrad.

Additionally, recent studies [19, 45, 27, 17, 21] proposed a plethora of evaluation metrics that incorporate human evaluation. Nevertheless, we adopt four metrics to assess the explanation performance, as they align with the two fundamental objectives of model explanation: model decisions [3, 37, 12, 16, 32] and human understanding [8, 43, 20, 6, 28]. **Consistency** [4] is primarily concerned with whether the explanation method is compatible with the learning capability of the model. **Invariance** [24] checks the explanation method to keep the output invariant in the case of constant data offsets in datasets with the same model architecture. **Sparseness** [10] measures whether the saliency map is distinguishable and identifiable. **Information Level** [22] measures the entropy of the saliency map.

5.1.2 Datasets and Models

To apply these metrics for comprehensive evaluation, referring to the setting in [24, 2], we choose MNIST [26] for experiments on **Consistency** and **Invariance**, ILSRCR2012 (ImageNet) [25] for experiments on **Sparseness** and **Information Level**.

Correspondingly, we construct a MLP model for **Consistency** and **Invariance** check, VGG16 [35], ResNet50 [18] and InceptionV3 [41] for visualization, **Sparseness** and **Information level** experiments. VGG16, ResNet50, and InceptionV3 are constructed by pre-trained models released in Torchvision². The MLP architecture consists of two linear layers with 200 and 10 units, respectively. The MLP was trained on MNIST by SGD optimizer with 20 epochs and the learning rate was set to 0.01.

5.1.3 Explanation methods

AdaptGrad, similar to SmoothGrad, is model-agnostic and can be applied to any gradient-based interpretability methods. Therefore, in addition to using smoothed gradients, we will also use AdaptGrad in combination with other methods to generate saliency maps for a more comprehensive evaluation. Due to the large number of gradient-based explanation methods, it is challenging to apply AdaptGrad to all of them. Thus, following [9] and [38], we select three different explanation methods for our experiments.

²<https://pytorch.org/vision/stable/index.html>

Gradient \times Input (GI) [36] is a simple explanation method that generates saliency maps by directly multiplying the image gradients with the input image. **GI** is the representative of the methods that directly use gradients to generate saliency maps. **Integrated Gradients (IG)** [40] generates saliency maps using global integrated gradients, which can avoid the gradient saturation problem. **IG** is the representative of the methods that partially use gradients in their computation. **IG** has different options for the baseline background. We have chosen black and white as the baseline backgrounds, which are labeled as **IG(B)** and **IG(W)** respectively. **NoiseGrad (NG)** [9] is another gradient smoothing method. However, unlike SmoothGrad and AdaptGrad, it reduces noise by perturbing model parameters, which introduces significant computational overhead and does not substantially improve the visualization quality. **NG** represents other gradient smoothing methods. We use the prefixes **S-** and **A-** to respectively denote the combination of SmoothGrad and AdaptGrad with other methods. **Grad**, **SG**, and **AG** denote the original gradient, SmoothGrad, and AdaptGrad.

Referring to the setup in [2, 24, 9], **Consistency** and **Invariance** are employed to validate SmoothGrad, AdaptGrad and their combinations with **NG**. And **Sparseness** is applied to evaluate all the explanation methods. Since **Information Level** is employed in methods of the **IGs** [22, 23, 44, 8], we use this metric when evaluating **IG**.

5.2 Qualitative Evaluation

As shown in Figure 5, we select a few examples to compare the visualization effects of SmoothGrad and AdaptGrad with different sampling number N . It is evident that the saliency maps generated by AdaptGrad exhibit superior visualization performance compared to SmoothGrad, particularly in terms of the presentation of object details. Even when $N = 10$, AdaptGrad could exhibit a clear noise reduction capability.

In Figure 6, we present an example of saliency maps generated by the combination of SmoothGrad and AdaptGrad with **GI**, **IG(B)**, **IG(W)** and **NG**. The results demonstrate that AdaptGrad exhibits a clear advantage over SmoothGrad in terms of the visualization of latent features, offering a more nuanced and detailed representation. Furthermore, the enhancement effect of AdaptGrad on the **IG** method is obvious, with a notable noise reduction in the saliency map and the presentation of intricate detail features, such as those pertaining to the facial features of a red fox.

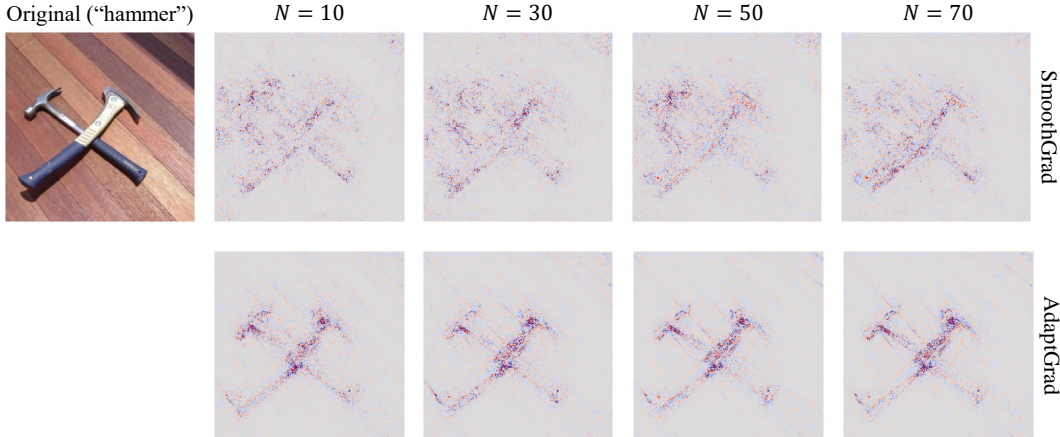


Figure 5: The visual saliency map from VGG16 of SmoothGrad and AdaptGrad with different sample times N .

5.3 Quantitative Evaluation

The settings outlined in Subsection 5.1 are employed to initially assess the consistency and invariance of AdaptGrad. The metric values are evaluated to ascertain whether they exhibit any aberrant deviations compared to the original gradients. The results of this assessment are reported in Table 1. It is evident that both AdaptGrad and SmoothGrad fall within the normal range on **Consistency** and **Invariance**, thereby indicating that AdaptGrad passes the checks for these two metrics.

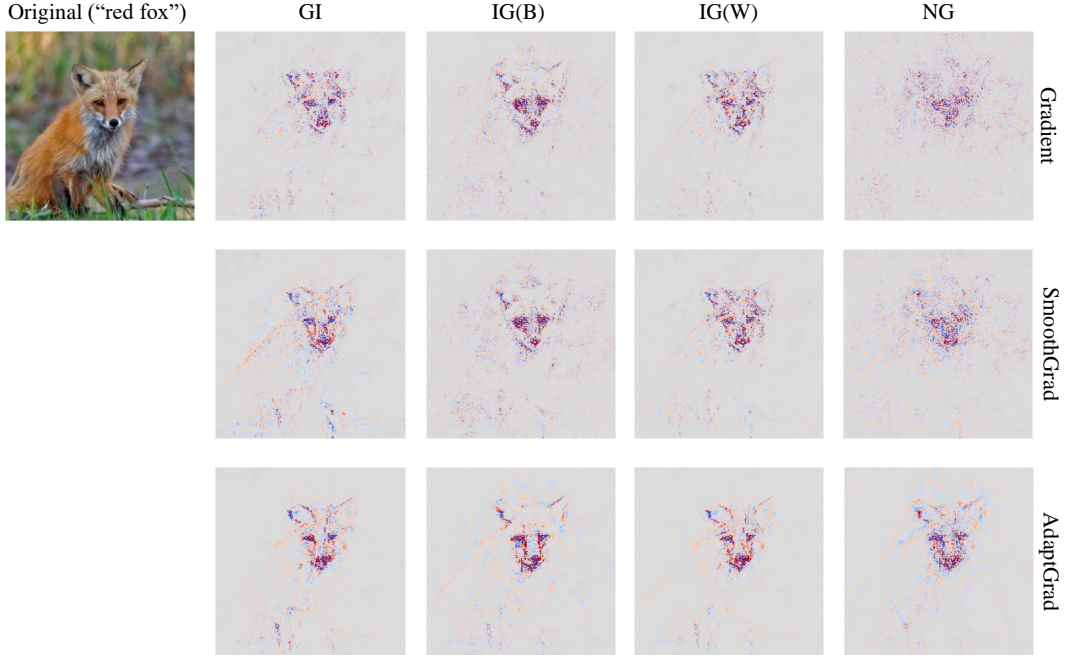


Figure 6: The visual saliency map from VGG16 of Gradient, SmoothGrad, and AdaptGrad combined with **GI**, **IG(B)**, **IG(W)** and **NG**.

Table 1: Results of **Consistency** and **Invariance** checks for SmoothGrad (**SG**) and AdaptGrad (**AG**)

Methods	Grad	SG	AG	NG	S-NG	A-NG
Consistency	0.0209	0.0189	0.0203	0.0209	0.0190	0.0202
Invariance	0.3483	0.3625	0.3480	0.3483	0.3615	0.3485

Table 2 reveals that the AdaptGrad method demonstrates notable superiority in the evaluation of **Sparseness** and **Information Level**. In terms of the Sparseness, the AdaptGrad method demonstrated a clear advantage over the SmoothGrad method in tests conducted across all three models and five types of interpretability methods with only one case slightly worse than the baselines. For the Information Level, the AdaptGrad method also mostly outperforms the SmoothGrad method. However, these metrics are based on certain assumptions about the quantitative analysis of visualization effects, and thus can only indirectly evaluate the performance of interpretability methods.

6 Conclusion

In this paper, we rethink the principles of gradient smoothing methods using the convolution formula, thereby defining the presence of inherent noise in gradient smoothing. Based on these analyzes, we design an adaptive gradient smoothing method, AdaptGrad, which can mitigate inherent noise. Theoretical analyzes of inherent noise, along with qualitative and quantitative experiments, demonstrate that AdaptGrad is a qualified alternative gradient smoothing method compared to SmoothGrad. In terms of implementation, AdaptGrad, like SmoothGrad, is computationally efficient and model-agnostic, and can be combined with other gradient-based explanation methods to enhance their performance.

Limitations and Future work

Optimization of inherent noise. Although we have formally defined the existence of inherent noise, it is evident that the symmetric characteristics of the Gaussian kernel hinder further optimization. We are only able to select the "shortest edge" as the confidence interval to regulate the σ of the Gaussian kernel, thereby ignoring the "longer edge". Thus, AdaptGrad might retain more gradient noise.

Table 2: Results of **Sparseness (SS)** and **Information Level (IL)** evaluation for SmoothGrad (**SG**), AdaptGrad (**AG**), and their combination with **GI**, **IG**, and **NG**. The \uparrow indicates the higher is better.

Methods	VGG16		InceptionV3		ResNet50	
	SS(\uparrow)	IL(\uparrow)	SS(\uparrow)	IL(\uparrow)	SS(\uparrow)	IL(\uparrow)
Grad	0.5421	-	0.5546	-	0.5626	-
SG	0.5334	-	0.5422	-	0.5536	-
AG	0.5608	-	0.5621	-	0.5659	-
GI	0.6198	-	0.6152	-	0.6304	-
S-GI	0.6074	-	0.5994	-	0.6176	-
A-GI	0.6487	-	0.6425	-	0.6479	-
IG(W)	0.6284	0.5635	0.7083	0.6677	0.6178	0.5491
S-IG(W)	0.6229	0.5741	0.7562	0.7179	0.6171	0.5718
A-IG(W)	0.6327	0.5846	0.7586	0.7221	0.6205	0.5849
IG(B)	0.6391	0.5823	0.6348	0.6751	0.6288	0.5355
S-IG(B)	0.6371	0.6035	0.6392	0.7166	0.6250	0.5731
A-IG(B)	0.6397	0.6121	0.6439	0.7193	0.6266	0.5673
NG	0.5519	-	0.5566	-	0.5626	-
S-NG	0.5551	-	0.5734	-	0.5591	-
A-NG	0.5823	-	0.5917	-	0.5738	-

The Selection of hyperparameters. In fact, the confidence t in AdaptGrad is still an "empirical" choice, despite its widespread use in the field of probability theory. As illustrated by Equation 5, t is a variable to balance the inherent noise and the gradient noise. Therefore, optimising the balance between these two factors may yield a more reasonable value.

References

- [1] A. Abid, M. Yuksekgonul, and J. Zou. Meaningfully debugging model mistakes using conceptual counterfactual explanations. In *International Conference on Machine Learning*, pages 66–88. PMLR, 2022.
- [2] J. Adebayo, J. Gilmer, M. Muelly, I. Goodfellow, M. Hardt, and B. Kim. Sanity checks for saliency maps. *Advances in neural information processing systems*, 31, 2018.
- [3] J. Adebayo, M. Muelly, I. Liccardi, and B. Kim. Debugging tests for model explanations. *Advances in Neural Information Processing Systems*, 33:700–712, 2020.
- [4] D. Alvarez Melis and T. Jaakkola. Towards robust interpretability with self-explaining neural networks. *Advances in neural information processing systems*, 31, 2018.
- [5] M. Ancona, E. Ceolini, C. Öztireli, and M. Gross. Towards better understanding of gradient-based attribution methods for deep neural networks. In *6th International Conference on Learning Representations (ICLR)*. Arxiv-Computer Science, 2018.
- [6] L. Arras, A. Osman, and W. Samek. Clevr-xai: A benchmark dataset for the ground truth evaluation of neural network explanations. *Information Fusion*, 81:14–40, 2022.
- [7] S. Bach, A. Binder, G. Montavon, F. Klauschen, K.-R. Müller, and W. Samek. On pixel-wise explanations for non-linear classifier decisions by layer-wise relevance propagation. *PLoS one*, 10(7):e0130140, 2015.
- [8] O. Barkan, Y. Asher, A. Eshel, N. Koenigstein, et al. Visual explanations via iterated integrated attributions. In *Proceedings of the IEEE/CVF International Conference on Computer Vision*, pages 2073–2084, 2023.
- [9] K. Bykov, A. Hedström, S. Nakajima, and M. M.-C. Höhne. Noisegrad—enhancing explanations by introducing stochasticity to model weights. In *Proceedings of the AAAI Conference on Artificial Intelligence*, volume 36, pages 6132–6140, 2022.
- [10] P. Chalasani, J. Chen, A. R. Chowdhury, X. Wu, and S. Jha. Concise explanations of neural networks using adversarial training. In *International Conference on Machine Learning*, pages 1383–1391. PMLR, 2020.
- [11] A. Chattopadhyay, A. Sarkar, P. Howlader, and V. N. Balasubramanian. Grad-cam++: Generalized gradient-based visual explanations for deep convolutional networks. In *2018 IEEE winter conference on applications of computer vision (WACV)*, pages 839–847. IEEE, 2018.

- [12] J. Crabbe, Y. Zhang, W. Zame, and M. van der Schaar. Learning outside the black-box: The pursuit of interpretable models. *Advances in neural information processing systems*, 33:17838–17849, 2020.
- [13] A.-K. Dombrowski, M. Alber, C. Anders, M. Ackermann, K.-R. Müller, and P. Kessel. Explanations can be manipulated and geometry is to blame. *Advances in neural information processing systems*, 32, 2019.
- [14] F. Doshi-Velez and B. Kim. Towards a rigorous science of interpretable machine learning. *arXiv preprint arXiv:1702.08608*, 2017.
- [15] M. Du, N. Liu, Q. Song, and X. Hu. Towards explanation of dnn-based prediction with guided feature inversion. In *Proceedings of the 24th ACM SIGKDD International Conference on Knowledge Discovery & Data Mining*, pages 1358–1367, 2018.
- [16] Z. T. Fernando, J. Singh, and A. Anand. A study on the interpretability of neural retrieval models using deepshap. In *Proceedings of the 42nd international ACM SIGIR conference on research and development in information retrieval*, pages 1005–1008, 2019.
- [17] T. Han, S. Srinivas, and H. Lakkaraju. Which explanation should i choose? a function approximation perspective to characterizing post hoc explanations. *Advances in Neural Information Processing Systems*, 35:5256–5268, 2022.
- [18] K. He, X. Zhang, S. Ren, and J. Sun. Deep residual learning for image recognition. In *Proceedings of the IEEE conference on computer vision and pattern recognition*, pages 770–778, 2016.
- [19] A. Hedström, L. Weber, D. Krakowczyk, D. Bareeva, F. Motzkus, W. Samek, S. Lapuschkin, and M. M.-C. Höhne. Quantus: An explainable ai toolkit for responsible evaluation of neural network explanations and beyond. *Journal of Machine Learning Research*, 24(34):1–11, 2023.
- [20] R. Ibrahim and M. O. Shafiq. Augmented score-cam: High resolution visual interpretations for deep neural networks. *Knowledge-Based Systems*, 252:109287, 2022.
- [21] P.-T. Jiang, C.-B. Zhang, Q. Hou, M.-M. Cheng, and Y. Wei. Layercam: Exploring hierarchical class activation maps for localization. *IEEE Transactions on Image Processing*, 30:5875–5888, 2021.
- [22] A. Kapishnikov, T. Bolukbasi, F. Viégas, and M. Terry. Xrai: Better attributions through regions. In *Proceedings of the IEEE/CVF international conference on computer vision*, pages 4948–4957, 2019.
- [23] A. Kapishnikov, S. Venugopalan, B. Avci, B. Wedin, M. Terry, and T. Bolukbasi. Guided integrated gradients: An adaptive path method for removing noise. In *Proceedings of the IEEE/CVF conference on computer vision and pattern recognition*, pages 5050–5058, 2021.
- [24] P.-J. Kindermans, S. Hooker, J. Adebayo, M. Alber, K. T. Schütt, S. Dähne, D. Erhan, and B. Kim. The (un) reliability of saliency methods. *Explainable AI: Interpreting, explaining and visualizing deep learning*, pages 267–280, 2019.
- [25] A. Krizhevsky, I. Sutskever, and G. E. Hinton. Imagenet classification with deep convolutional neural networks. *Advances in neural information processing systems*, 25, 2012.
- [26] Y. LeCun and C. Cortes. The mnist database of handwritten digits, 2005. URL <https://api.semanticscholar.org/CorpusID:60282629>. Last accessed on 2024-05-22.
- [27] Y. Liu, H. Li, Y. Guo, C. Kong, J. Li, and S. Wang. Rethinking attention-model explainability through faithfulness violation test. In *International Conference on Machine Learning*, pages 13807–13824. PMLR, 2022.
- [28] Y. Y. Lu, W. Guo, X. Xing, and W. S. Noble. Dance: Enhancing saliency maps using decoys. In *International Conference on Machine Learning*, pages 7124–7133. PMLR, 2021.
- [29] G. Montavon, S. Lapuschkin, A. Binder, W. Samek, and K.-R. Müller. Explaining nonlinear classification decisions with deep taylor decomposition. *Pattern recognition*, 65:211–222, 2017.
- [30] M. Nauta, J. Trienes, S. Pathak, E. Nguyen, M. Peters, Y. Schmitt, J. Schlötterer, M. van Keulen, and C. Seifert. From anecdotal evidence to quantitative evaluation methods: A systematic review on evaluating explainable ai. *ACM Computing Surveys*, 55(13s):1–42, 2023.
- [31] W. Nie, Y. Zhang, and A. Patel. A theoretical explanation for perplexing behaviors of backpropagation-based visualizations. In *International conference on machine learning*, pages 3809–3818. PMLR, 2018.

- [32] W. Samek, A. Binder, G. Montavon, S. Lapuschkin, and K.-R. Müller. Evaluating the visualization of what a deep neural network has learned. *IEEE transactions on neural networks and learning systems*, 28(11): 2660–2673, 2016.
- [33] R. R. Selvaraju, M. Cogswell, A. Das, R. Vedantam, D. Parikh, and D. Batra. Grad-cam: Visual explanations from deep networks via gradient-based localization. In *Proceedings of the IEEE international conference on computer vision*, pages 618–626, 2017.
- [34] A. Shrikumar, P. Greenside, and A. Kundaje. Learning important features through propagating activation differences. In *International conference on machine learning*, pages 3145–3153. PMLR, 2017.
- [35] K. Simonyan and A. Zisserman. Very deep convolutional networks for large-scale image recognition. *arXiv preprint arXiv:1409.1556*, 2014.
- [36] K. Simonyan, A. Vedaldi, and A. Zisserman. Deep inside convolutional networks: visualising image classification models and saliency maps. In *Proceedings of the International Conference on Learning Representations (ICLR)*. ICLR, 2014.
- [37] L. Sixt, M. Granz, and T. Landgraf. When explanations lie: Why many modified bp attributions fail. In *International Conference on Machine Learning*, pages 9046–9057. PMLR, 2020.
- [38] D. Smilkov, N. Thorat, B. Kim, F. Viégas, and M. Wattenberg. Smoothgrad: removing noise by adding noise. *arXiv preprint arXiv:1706.03825*, 2017.
- [39] J. Springenberg, A. Dosovitskiy, T. Brox, and M. Riedmiller. Striving for simplicity: The all convolutional net. In *ICLR (workshop track)*, 2015.
- [40] M. Sundararajan, A. Taly, and Q. Yan. Axiomatic attribution for deep networks. In *International conference on machine learning*, pages 3319–3328. PMLR, 2017.
- [41] C. Szegedy, V. Vanhoucke, S. Ioffe, J. Shlens, and Z. Wojna. Rethinking the inception architecture for computer vision. In *Proceedings of the IEEE conference on computer vision and pattern recognition*, pages 2818–2826, 2016.
- [42] H. Wang, Z. Wang, M. Du, F. Yang, Z. Zhang, S. Ding, P. Mardziel, and X. Hu. Score-cam: Score-weighted visual explanations for convolutional neural networks. In *Proceedings of the IEEE/CVF conference on computer vision and pattern recognition workshops*, pages 24–25, 2020.
- [43] Y. Wu, C. Chen, J. Che, and S. Pu. Fam: Visual explanations for the feature representations from deep convolutional networks. In *Proceedings of the IEEE/CVF Conference on Computer Vision and Pattern Recognition*, pages 10307–10316, 2022.
- [44] R. Yang, B. Wang, and M. Bilgic. Idgi: A framework to eliminate explanation noise from integrated gradients. In *Proceedings of the IEEE/CVF Conference on Computer Vision and Pattern Recognition*, pages 23725–23734, 2023.
- [45] S. C.-H. Yang, N. E. T. Folke, and P. Shafto. A psychological theory of explainability. In *International Conference on Machine Learning*, pages 25007–25021. PMLR, 2022.
- [46] C.-K. Yeh, C.-Y. Hsieh, A. Suggala, D. I. Inouye, and P. K. Ravikumar. On the (in) fidelity and sensitivity of explanations. *Advances in Neural Information Processing Systems*, 32, 2019.
- [47] M. D. Zeiler and R. Fergus. Visualizing and understanding convolutional networks. In *Computer Vision—ECCV 2014: 13th European Conference, Zurich, Switzerland, September 6–12, 2014, Proceedings, Part I 13*, pages 818–833. Springer, 2014.
- [48] L. Zhou, X. Shi, Y. Bao, L. Gao, and C. Ma. Explainable artificial intelligence for digital finance and consumption upgrading. *Finance Research Letters*, 58:104489, 2023.